Numerical validation of a simplified design procedure for calculating the heating load in buildings with Breathing Wall components

Andrea Alongi[1], Adriana Angelotti[1], Livio Mazzarella[1]
[1]Politecnico di Milano, Milano, Italy

Abstract

Breathing Walls (BWs) can provide significant building energy saving in winter conditions, but the present standard methodology for heating load calculation fails to consider this technology, thus limiting its application. In this paper, a procedure to include BWs in the EN 12831-1:2017 is then proposed. The methodology is tested against a numerical calculation of the heating load based on the coupling between the Building Energy Simulation (BES) engine TRNSYS and a Matlab Finite Difference Model (FDM) addressing heat and mass transfer across the BW. The very good agreement demonstrates that the BW can be syntethized by two key parameters, namely the effective thermal transmittance at the interior surface and the thermal recovery efficiency.

Highlights

- New methodology to include Breathing Walls in standard heating load calculation.
- Analytical approach validated against detailed numerical simulations.
- Effective U-value at the internal surface and thermal heat recovery are the key BW parameters for design heat load calculation.
- Effective U-value at the external surface is the key parameter for checking the limits imposed by regulatory standards.

Introduction

Among the advanced building envelope technologies, Breathing Walls (BW), originally known as Dynamic Insulation, are a promising approach to reduce energy needs. According to Imbabi (2012) BWs are permeodynamic components based on air permeable layers that are crossed by the controlled ventilation airlfow, either in supply or extraction mode. Depending on the direction of heat flux and airflow, two working regimes can be identified: *contra-flux* when they have opposite directions and *pro-flux* when they have the same direction (Taylor et al., 1996; Alongi et al., 2017).

Early research on BWs was mainly focused on winter performance, where the contra-flux regime is shown to be the most effective: the air entering through the wall is preheated and transmission heat losses toward the outdoor are reduced. In Brunsell (1995) it is shown that the dynamic or effective U-value of the wall decreases when the speed of the airflow that crosses it increases, and the dynamic U-value is operatively defined as the U-value of a construction with traditional insulation with the same heat losses as the Dynamic Insulation one. It is important to notice that only one-layer construction are considered and the effects of surface resistances are neglected.

More recently, the interest has also been dedicated to the effects of BW on the cooling performance of buildings (Elsarrag, 2012; Imbabi, 2012; Zhang et al., 2019; Alongi et al., 2021b) and both pro and contra flux conditions have been investigated.

However, even though in recent years dynamic insulation components, such as BW, have been subject to growing interest in the scientific community (Karanafti et al., 2022), the technical standards currently in use by designers are not able to fully consider the features of these technologies. This means that engineers and architects, being forced to fulfill requirements on several parameters (e.g.: thermal transmittance of envelope components), cannot optimize the buildings and facilities design, potentially leading to excessive insulation or oversizing of the heating generation system. Moreover, in the scientific literature dedicated to BWs, parameters such as the effective thermal transmittance or the heat recovery efficiency are only discussed in the context of a single fully permeable component, while their definition for more general components (including both permeable and non permeable layers) and their use in the assessment of the thermal balance of an enclosed space are not investigated.

Therefore, the purpose of the paper is to define and test a design heat load calculation procedure for buildings involving BW components, that implements the same approach presented in the technical standards currently in force (EN 12831-1:2017).

Since the focus is oriented toward winter conditions, only the contra-flux regime achievd through mechanical ventilation is considered in this work.

Methods

In this work, a procedure to include BW technology in the standard heating load calulation (EN 12831-1:2017), by identifying the BW key thermal-physical parameters, is firstly defined. Subsequently this approach is tested against numerical simulations where the heat and mass transfer through the BW component is explicitely modelled and the thermal zone heating load is obtained from the resulting losses in steady state regime. The

https://doi.org/10.26868/25222708.2023.1599

simulations are performed on a virtual case study modeled in TRNSYS 18 and connected to a Matlab Finite Difference Model (FDM) aimed at BW heat transfer simulation. The ultimate purpose is then to find reference parameters useful to designers as a tool to compare BWs to traditional components and to assess their performance and efficacy.

The heating load calculation including BW technology

According to the standard EN 12831-1:2017, the design heat load Φ_{HL} for a generic heated space is calculated as:

$$\Phi_{HL} = \Phi_T + \Phi_V + \Phi_{hu} - \Phi_{gain} \quad (1)$$

where Φ_T and Φ_V are the design transmission and ventilation heat losses respectively, Φ_{hu} is the optional additional heating up power for intermittent heating and Φ_{gain} are the optional heat gains. Since BW components are at the same time part of the building envelope and part of the mechanical ventilation system, they affect both transmission and ventilation losses. If any BW component is present, we propose to generalise the transmission losses as follows:

$$\Phi_T = \Phi_{T,NP} + \Phi_{T,BW} + \Phi_{TB} \quad (2)$$

where $\Phi_{T,NP}$ are the transmission losses through conventional non-permeable components, Φ_{TB} are transmission losses due to thermal bridges and $\Phi_{T,BW}$ are those through BW components. Considering for simplicity only a single BW, they are calculated as:

$$\Phi_{T,BW} = A_{BW} \cdot U_{BW,x} \cdot \left(T_{des,i} - T_{des,e}\right) \quad (3)$$

where $T_{des,i}$ and $T_{des,e}$ are the internal and external design temperatures, A_{BW} is the frontal area of the external BW and $U_{BW,x}$ is the corresponding thermal transmittance. The latter was initially introduced in the pioneering work by (Taylor and Imbabi, 1998) and adopted in subsequent studies (Dimoudi et al., 2004; Imbabi, 2006; Imbabi, 2012), although mainly used to assess the performance of the component itself. When it comes to a thermal zone energy balance, it has to be remarked that for a BW the heat flux densities at the outdoor and at the indoor surfaces are different, as shown empirically by Baker (2003), because the conductive heat flux increases when passing from outside to inside. Therefore, two values of *effective* thermal transmittance $U_{BW,e}$ (external) and $U_{BW,i}$ (internal) can in principle be defined, namely:

$$U_{BW,e} = \frac{\varphi_e}{(T_{des,i} - T_{des,e})} \quad (4)$$

and

$$U_{BW,i} = \frac{\varphi_i}{(T_{des,i} - T_{des,e})} \quad (5)$$

where φ_e and φ_i are the heat flux densities at the external and at the internal surfaces of the BW component respectively. A similar distinction is found in Elsarrag et al. (2012), although the two U-values are referred to the surface temperatures and not to the operative temperatures, in fact representing the thermal conductances. Most of the works from literature only discuss the U-value referred to the outer surface (Taylor et al., 1998; Imbabi, 2006; Imbabi, 2012). In this work we calculate both and confront their suitability for heating load calculations.

Concerning ventilation losses, we propose to include the BW by referring to the case of mechanical ventilation with heat recovery, namely:

$$\Phi_V = \left(\rho c_p\right)_f \cdot \dot{V}_{sup} \cdot \left(T_{des,i} - T_{rec}\right) \quad (6)$$

where $\dot{V}_{sup}$ is the supply volume airflow rate for the thermal zone, defined as the product between the airchange rate n and the net volume of the zone V, ρ and c_p are the density and specific heat at constant pressure of air (f), and T_{rec} is the air temperature after passing through the heat recovery system. Since the BW behaves as a heat recovery heat exchanger, T_{rec} is the temperature of air entering the indoor environment from the BW system, later in this paper referred to as $T_{cav,BW}$. Moreover, it is possible to use the heat recovery efficiency of the BW system introduced by Alongi et al. (2020) as:

$$\eta_{BW} = \frac{T_{cav,BW} - T_{des,e}}{T_{des,i} - T_{des,e}} \quad (7)$$

turning then Eq. (6) into:

$$\Phi_V = \left(\rho c_p\right)_f \cdot \dot{V}_{sup} \cdot (1 - \eta_{BW}) \cdot \left(T_{des,i} - T_{des,e}\right) \quad (8)$$

Remarkably, the proposed methodology identifies the thermal transmittance $U_{BW,x}$ and the heat recovery efficiency η_{BW} as the key parameters of a BW component that allow to calculate the heating load.

The BW numerical model

The Finite Difference Model, presented and validated in Alongi et al. (2021a), to simulate one-dimensional BW layers is based on the modified Fourier equation:

$$(\rho c)_w \frac{\partial T}{\partial t} + u_f \left(\rho c_p\right)_f \frac{\partial T}{\partial x} = \lambda_w \frac{\partial^2 T}{\partial x^2} \quad (9)$$

where T is the time-dependent temperature distribution, u_f is the airflow velocity across the wall (positive when moving inward, negative when moving outward) and ρ, c and λ are the density, the specific heat (at constant pressure when the p subscript is added) and the thermal conductivity of porous material (subscript w) or air (subscript f).

The FDM deals with the time variable using the Backward Euler approach, while the spatial derivatives (second order for diffusion and first order for advection) are approximated with the adequate central difference scheme. In Alongi et al. (2021b) the algorithm has been provided with the ability to deal with multi-layer domains of both permeable and non-permeable materials, and of ventilated and non-ventilated cavities. The latter are treated considering the temperature dependence of the convective and radiative heat exchange through an iterative approach. For more details about these features, please refer to Alongi et al. (2021b).

Robin boundary conditions, along with an imposed heat flux, are still considered for the outer edge of the domain, while for the inner one Dirichlet bondary conditions are used in this work to improve the integration in the TRNSYS model, as discussed below.

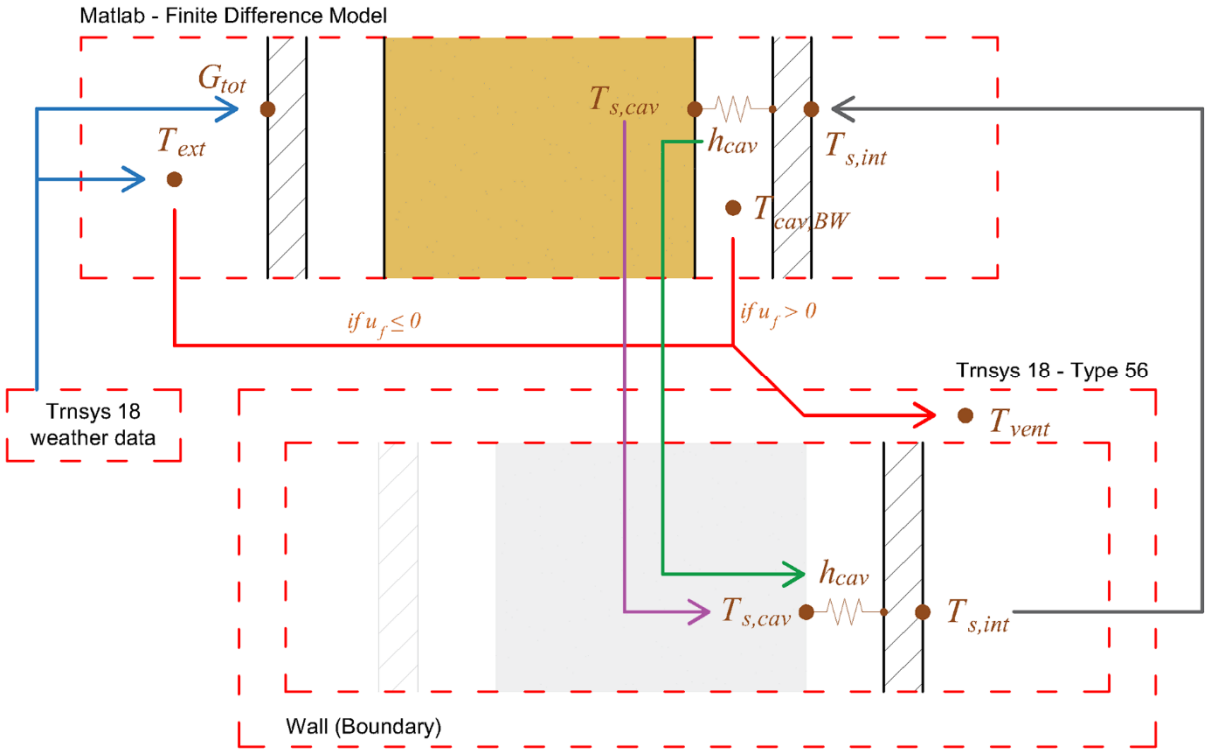

Figure 1:coupling scheme between the Matlab FDM algorithm and the building model in TRNSYS 18.

Improved coupling between the FDM and TRNSYS

As described in the previous work (Alongi et al., 2021b), the Matlab Finite Difference Model is linked to the TRNSYS 18 Multi-Zone Building model (Type 56) through the Type 155, dedicated to calling external Matlab scripts.

In this study the connection between these two parts of the model has been modified, in order to allow the use of the standard starnet radiation model on the indoor side, which was not implemented previously and was substituted with the simplified one node model.

The coupling between the TRNSYS Building Model and the BW FDM is still based on a recursive approach (Figure 1). Only the innermost layer of the wall is defined inside the TRNSYS Building Model. This layer is set as a "Boundary" surface provided with user-defined external temperature and surface heat transfer coefficiens. These two quantities are calculated by the FDM, where in turn the entire wall domain is modelled, and they correspond to the temperature of the outer surface of the porous layer ($T_{s,cav}$) and to the convective-radiative heat transfer coefficient (h_{cav}) of the innermost cavity. If the airflow is directed inward through the BW, the FDM also provides the average temperature of this innermost cavity ($T_{cav,BW}$), which is used as supply temperature for the ventilation in the TRNSYS building model. At the same time, the FDM uses the weather data provided by TRNSYS (air temperature and total incident radiation) as outdoor boundary conditions. Unlike in the previous work, the FDM does not use the internal node temperature as indoor boundary condition, but the internal surface temperature of the corresponding wall (namely, the single layer "Boundary" wall previously discussed). In this way, the building model in TRNSYS is able to calculate the longwave radiation exchange within a zone using the standard starnet mode, as mentioned before.

The building model

The building model considered as a case study is made of a single thermal zone with a floor area of 25 m^2, an internal air volume of 75 m^3 and an external BW of 15 m^2, defined according to the layer sequence represented in Figure 2 and Table 1. In order to isolate the effects of the BW component on the energy balance, all other surfaces of the thermal zone are considered adiabatic. Following the previous discussion, only layer 7 (plasterboard) is modeled inside TRNSYS, and its external boundary conditions provided by the FDM are the temperature of the external surface and the convective-radiative heat transfer coefficient of the non-ventilated cavity (layer 6). As far as the thickness of the air permeable insulation layer s_{ins} is concerned, two values of 5 cm and 10 cm are considered alternatively. The BW is assumed to operate in *contra-flux* regime, the most suitable for winter conditions (Taylor and Imbabi, 1998; Alongi et al., 2017). Therefore, the air flows from outdoor to indoor being pre-heated by the BW. As shown in Table 2, different airflow velocities u_f are considered, leading to different airchange rates n for the indoor environment.

Coherently with the Italian heating load calculation practice, no internal gains due to people activity, light or appliances are considered for the thermal zone and solar radiation is considered null. Moreover, since the procedure described by the EN 12831-1:2017 is based on a steady-state approach, external temperatures (dry bulb

https://doi.org/10.26868/25222708.2023.1599

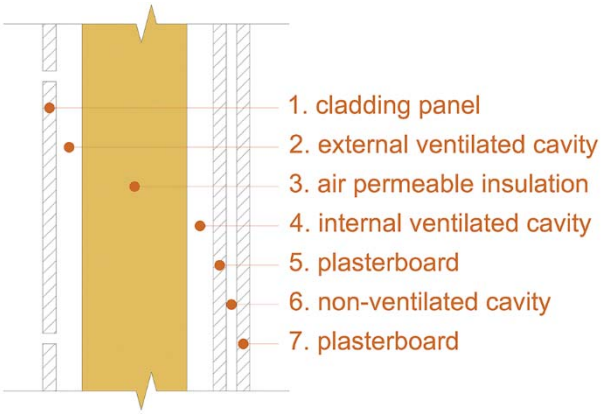

Figure 2:the layer sequence of the BW component.

Table 1: geometrical and physical properties of the layers in the BW.

ID	s [m]	λ [W/(m.K)]	ρ [kg/m³]	c [J/(kg.K)]
1	0.025	0.35	1150	1000
2	0.05	-	-	-
3	s_{ins}	0.034	50	1030
4	0.05	-	-	-
5	0.025	0.25	1000	1000
6	0.02	-	-	-
7	0.025	0.25	1000	1000

Table 2: airchange rates considered in the TRNSYS building model and corresponding airflow velocities.

ID	n [h^{-1}]	u_f [m/s]
AF1	0.36	0.0005
AF2	0.72	0.001
AF3	1.44	0.002
AF4	3.60	0.005

air temperature, effective sky temperature and effective ground temperature) are set to the constant value of -5 °C, namely the design external operative temperature value for Milan (Italy) according to the UNI/TR 10349-2:2016. Finally, the optional additional heating up power for intermittent heating Φ_{HL} is considered null. As far as indoor conditions are concerned, a set point temperature equal to 20°C is assumed for the ideal heating plant. It is important to notice that TRNSYS only allows to control the air temperature of the thermal zone. On the other hand, the technical EN 12831-1:2017 assumes the same internal design temperature for both transmission and ventilation heat losses, therefore conflating in a single quantity indoor operative and air temperatures. This issue will be discussed later.

Even though boundary conditions are constant, it is necessary to reach steady state, so that simulations are run for 1416 timesteps of 1 hour, corresponding to the period of January and February. When the main variables reach constant values, the relevant outputs are extracted, namely: the sensible thermal heating load $\dot{Q}_{sens}$ [W], the transmission heat losses $\dot{Q}_T$ [W] and the ventilation heat losses $\dot{Q}_V$ [W], along with the operative temperature of the thermal zone $T_{op,i}$. $\dot{Q}_{sens}$ is then confronted to Φ_{HL} (Eq. 1) obtained from the standard heating load calculation, modified as previously described to include the BW components. In order to calculate the key parameters of the BW, namely the external and internal U-value (Eq. 4 and 5) and the heat recovery efficiency η_{BW} (Eq. 7) the FDM is used. More in detail, the two heat flux densities are calculated using the solution of the FDM through a three-points formulation as:

$$\varphi_e = \lambda_1 \frac{3T_1 - 4T_2 + T_3}{2\Delta x_1} \quad (10)$$

$$\varphi_i = -\lambda_M \frac{3T_N - 4T_{N-1} + T_{N-2}}{2\Delta x_M} \quad (11)$$

where λ_1 and λ_M are the thermal conductivity of the first and the last (M-th) layer of the BW component, Δx_1 and Δx_M are the corresponding space discretizations, T_1, T_2 and T_3 are the solutions at the first three nodes of the domain and T_{N-2}, T_{N-1} and T_N are the solutions at the last three nodes of the domain. Future efforts will be dedicated to the definition of equations for the analytical calculation of $U_{BW,e}$, $U_{BW,i}$ and η_{BW}, a crucial step for a full application of the proposed heating load calculation.

Results and Discussion

As first step, the two groups of simulation, corresponding to two kinds of BW with either 5 cm or 10 cm of porous insulation, each working at 4 different air flow velocities (Table 2), have been performed in TRNSYS. The trends for sensible heating load and for transmission and ventilation heat losses as a function of the air velocity through the BW have been achieved. Figure 3 shows that the insulation thickness becomes irrelevant for airchange rates above 1.44 h^{-1}: while at the lowest value 10 cm of insulation provide a 15 % reduction of sensible heating load over 5 cm, at higher airchange rates this quantity is dominated by the ventilation heat losses, that show fairly similar trends in the two groups. Moreover, in Figure 3(b) it is possible to observe that transmission heat losses grow with the airflow rates. This means that, since the area and the temperature difference in Eq.(3) are constant, the right U-value to be used in the heating load calculation is the one showing growing trend with increasing air velocity.

At the same time, the properties of the two BWs investigated have been numerically derived according to the previous description. Since the aim was to achieve general trends as function of u_f, a Matlab FDM algorithm separated from the one linked to TRNSYS has been used, in which third type boundary conditions are assumed on the indoor edge of the domain, setting the indoor and the outdoor temperatures at 20 °C and -5 °C respectively. The external and internal effective U-values are shown in Figure 4(a) and the heat recovery efficiencies are reported in Figure 4(b). From Figure 4(a) it can be noticed that the effective transmittance at the internal surfaces features a growing trend coherent with that of $\dot{Q}_T$ from the

https://doi.org/10.26868/25222708.2023.1599

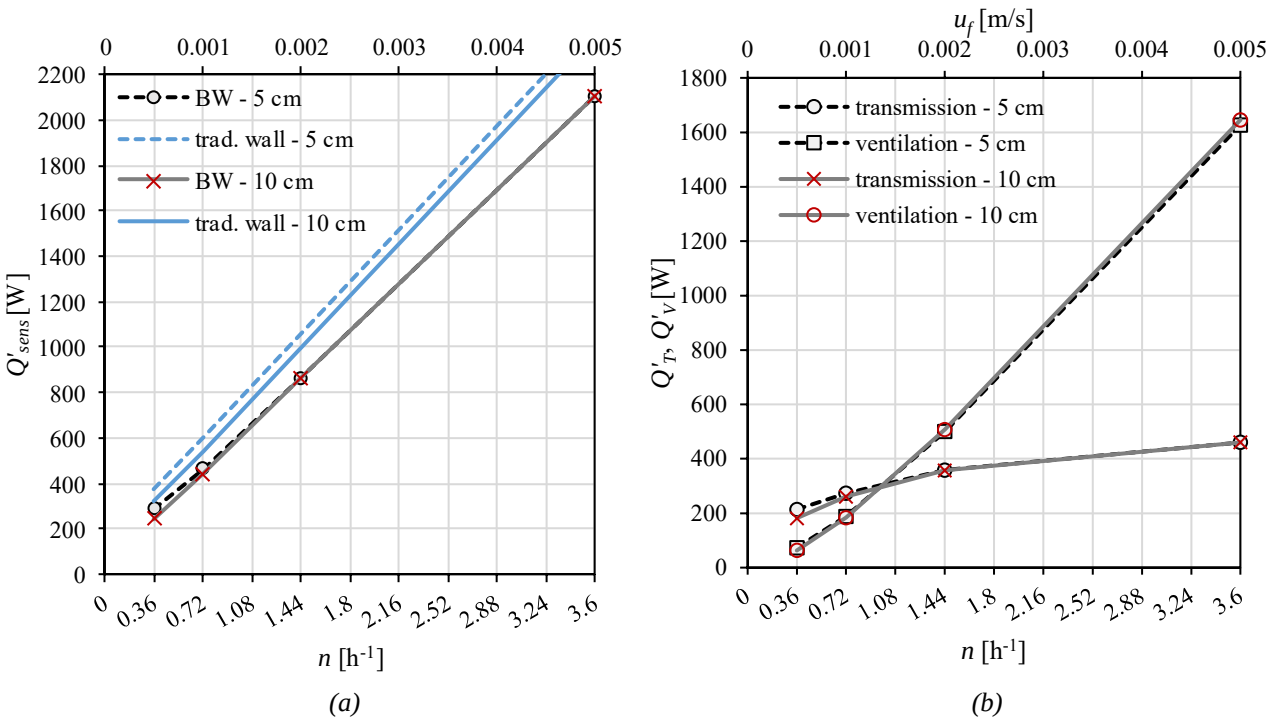

Figure 3: (a) sensible heating thermal load for the buildings with 5 cm or 10 cm insulation thickness, involving either BW components or traditional walls. (b) transmission and ventilation heat losses for the two building models provided with BWs.

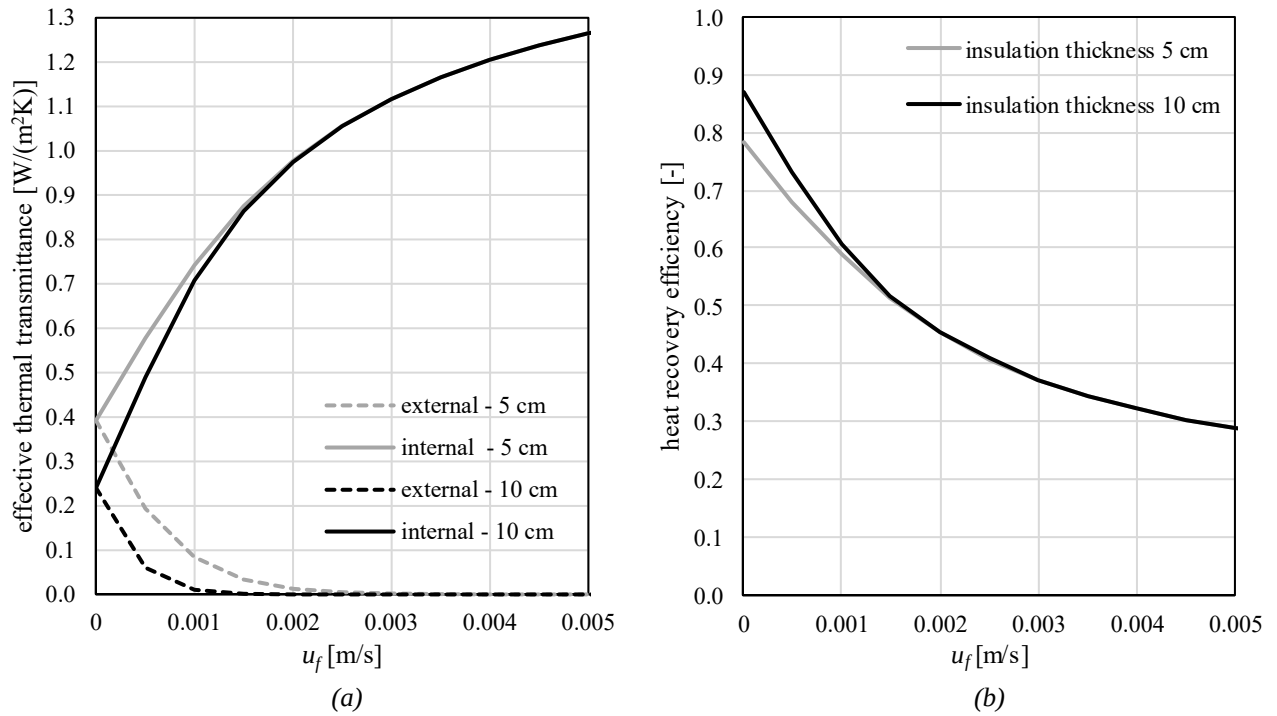

Figure 4: (a) internal and external thermal transmittance and (b) heat recovery efficiency for the two BWs. All quantities are provided as a function of the airflow velocity across the permeable layers.

simulations, while the U-value on the outdoor surface tends to zero. Therefore, the transmission losses in the heating load calculation should be based on $U_{BW,i}$.

Therefore, $U_{BW,i}$ and η_{BW} have then be used to calculate the design heat load as a sum of transmission and ventilation heat losses, according to the procedure presented previously, and the outcomes have been compared to the output of the corresponding simulations in Table 3. The three main outputs from the simulations

https://doi.org/10.26868/25222708.2023.1599

Table 3: comparison between the simulation results and the corresponding quantities calculated through the simplified method described in the EN 12831-1:2017.

	simulations			Eqs. (1), (2) and (3)		
n	$\dot{Q}_{sens}$	$\dot{Q}_T$	$\dot{Q}_V$	Φ_{HL}	Φ_T	Φ_V
[h^{-1}]	[W]	[W]	[W]	[W]	[W]	[W]
insulation thickness 5 cm						
0.36	289	214	75	290	217	73
0.72	466	274	193	462	274	188
1.44	868	358	509	859	359	500
3.6	2106	460	1646	2088	461	1627
insulation thickness 10 cm						
0.36	245	182	63	245	184	62
0.72	445	261	184	441	261	179
1.44	865	357	507	856	358	498
3.6	2106	460	1646	2088	461	1627

and the corrisponding quantities manually calculated using Eqs. (1), (3) and (7) show good agreement, with relative errors within 3 %. It is important to notice that the main source of discrepancy is related to two factors: first of all, TRNSYS uses different conditions for the indoor environment when dealing with transmission through the envelope (convection with air at 20 °C and starnet model for longwave radiation between surfaces) and ventilation (air temperature at 20 °C). On the contrary, the manual calculations have been performed assuming a general internal temperature of 20 °C for both components of the heat balance. Moreover, the FDM model does not consider the thermal resistance of airgaps in the wall domain as fixed, but it takes into account the non linearity of the heat transfer problem. Therefore, even a slight difference in the value for the internal boundary condition can introduce discrepancies. Indeed, if the internal operative temperature from the simulations is used to numerically derive the U-values and the heat recovery efficiency, as well as to solve Eq. (3) in place of $T_{des,i}$, the differences between the simulation outputs and the corresponding quantities calculated manually drop well below 0.001 %. Thus, the small errors observed in Table 3 when using a single internal temperature of 20 °C for both transmission and ventilation heat losses show that this simplified approach is consistent with the physics of the phenomena investigated, and that $U_{BW,i}$ and η_{BW} can reliably be used in the design heat load calculation process, as described by the standard EN 12831-1:2017. Therefore, even though the literature mostly considers as U-value for a BW component the one calculated on the outer surface (namely, $U_{BW,e}$ in this work), it does not have any practical use for heating load calculations. On the other hand, this quantity allows to calculate the energy lost to the outdoor environment and not recovered in any way. Therefore, since in a traditional wall the U-value actually represents the energy lost to the outdoor environment, $U_{BW,e}$ is the appropriate parameter to use to verify the thermal performance of a BW component against the limits mandated by local authorities.

The increasing trend of the losses for the thermal zone at increasing air velocity across the component should not lead to the wrong conclusion that the BW is useless or even counterproductive with respect to a traditional non-permeable wall. Along with $\dot{Q}_{sens}$ achieved for the two models involving BW technology, the same quantity referred to a traditional wall is shown as comparison in Figure 3(a): at any given value of n the latter is higher than the former. More in detail, the implementation of BW components allows a desing heating load reduction from a maximum of around 23 % (n = 0.36 h^{-1}), to a minimum of around 11 % (n = 3.60 h^{-1}). Indeed, as it was shown in Alongi et al. (2020), an optimal condition is obtained when air moves with the lowest possible velocity able to provide the overall airflow rate required, since it ensures the highest possible heat recovery efficiency (see Figure 4(b)), while minimizing the heat exchange with the wall (Figure 4(a)).

Conclusions

In this paper the possibility has been demonstrated to generalise the standard procedure for heating load calculation to buildings featuring BW components in the envelope. While a conventional wall is identified by its thermal transmittance, it was shown that a BW component can be identified as both an envelope component with an effective U-value and a mechanical ventilation component with a heat recovery efficiency. Testing this approach against numerical simulations where the heat and mass transfer across the BW is solved has shown a very good agreement, even when the distinction between operative temperature and air temperature is neglected. Morevoer, it was demonstrated that the appropriate parameter to calculate transmission heat losses is the effective thermal transmittance evaluated at the indoor surface $U_{BW,i}$, despite previous works from literature only presented the one calculated at the outdoor surface.

On the other hand, $U_{BW,e}$ becomes relevant when providing an indication of the thermal performance of a BW component and can be used to verify the compliance with the limits imposed by legislation.

Future research on BW technology will be focused on the definition of analytical procedures to evaluate the effective U-values and the heat recovery efficiency in walls with air permeable and non-permeable layers at the same time, also considering the convective-radiative heat transfer coefficients at both indoor and outdoor surfaces.

References

Alongi, A., Angelotti, A., Mazzarella, L. (2017). Experimental investigation of the steady state behaviour of Breathing Walls by means of a novel laboratory apparatus. *Building and Environment 123*, 415–426.

Alongi, A., Angelotti, A., Mazzarella, L. (2020). Measuring a Breathing Wall's effectiveness and

dynamic behaviour. *Indoor and Built Environment 29(6)*, 783–792.

Alongi, A., Angelotti, A., Mazzarella, L. (2021a). A numerical model to simulate the dynamic performance of Breathing Walls. *Journal of Building Performance Simulation 14*(2), 155–180.

Alongi, A., Angelotti, A., Mazzarella, L. (2021b). Investigating the control strategies for Breathing Walls during summer: a dynamic simulation study. *Proceedings of the 17th IBPSA Conference*. Bruges (BE), 1-3 September 2021.

Baker, P.H. (2003). The thermal performance of a prototype dynamically insulated wall. *Building Services Engineering Research and Technology 24(1)*, 25-34.

Brunsell, J.T. (1995). The performance of Dynamic Insulation in two residential buildings. *Air Infiltration Review 16(4)*, 7-11

Dimoudi, A., Androutsopoulos, A., Lykoudis, S. (2004). Experimental work on a linked, dynamic and ventilated, wall component. *Energy and Buildings 36*, 443-453.

Elsarrag, E., Al-Horr, Y., Imbabi, M.S. (2012). Improving building fabric energy efficiency in hot-humid climates using dynamic insulation. *Building Simulation 5*, 127-134.

Ente Italiano di Normazione (2016). *Riscaldamento e raffrescamento degli edifici – Dati climatici - Parte 2: Dati di progetto (UNI/TR 10349-2).*

European Committee for Standardisation (2017). *Energy performance of buildings - Method for calculation of the design heat load - Part 1: Space heating load, Module M3-3s (EN 12831-1).*

Imbabi, M.S. (2006). Modular breathing panels for energy efficient, healthy building construction. *Renewable Energy 31*, 729-738.

Imbabi, M.S. (2012). A passive–active dynamic insulation system for all climates. *International Journal of Sustainable Built Environment 1*, 247-258.

Karanafti, A., Theodosiou, T., Tsikaloudaki, K. (2022). Assessment of buildings' dynamic thermal insulation technologies - A review. *Applied Energy 326*, 119985.

Taylor, B.J., Imbabi, M.S. (1998) The application of Dynamic Insulation in Buildings. *Renewable Energy 15*, 377-382.

Taylor, B.J., Cawthorne, D.A., Imbabi, M.S. (1996) Analytical investigation of the steady-state behaviour of Dynamic and Diffusive building envelopes. *Building and Enuironment 31(6)*, 519-525.

Zhang, C., Wang J., Li L., Gang W. (2019). Dynamic thermal performance and parametric analysis of a heat recovery building envelope based on air-permeable porous materials. *Energy 189*, 116361.